REFRACTION INFLUENCE ANALYSIS AND INVESTIGATIONS ON AUTOMATED ELIMINATION OF REFRACTION EFFECTS ON GEODETIC MEASUREMENTS

***B. Böckem*[1], *P. Flach*[1], *A. Weiss*[2], *M. Hennes*[1]**
Swiss Federal Institute of Technology (ETH), Zurich, Switzerland
[1] Institute of Geodesy and Photogrammetry
[2] Institute of Geography

Abstract: Refraction effects are generally caused by an inhomogeneous propagation medium for the optical beam and are recognized as today's major source of systematic errors in the precise optical determination of angles and distances. Because meteorological point measurements do not deliver satisfactory correction values, the investigation of alternative methods motivated the development of a dispersometer, a metrological solution with a very sophisticated instrumental set-up. Furthermore, the compensation of deterministic refraction effects basing on atmospheric scintillation is envisaged: Optical scintillation measurements with a scintillometer or with CCD-sensors yield line averaged turbulence parameters of the atmospheric surface layer, which can be used for determining the refractive index gradient. Because CCD-sensors are implemented in today's high-end surveying instruments, automated on-board-solutions will be possible.

Keywords: Refraction, direction transfer, dispersion, dispersometry, scintillation, scintillometry, image analysis

1 INTRODUCTION

Geodetic measurements deliver mainly two- or three-dimensional geometric information of objects. These cover a wide range from the shape of the earth to industrial parts. In this paper we focus on geodetic measurements for construction and monitoring tasks spanning over several hundred meters: here usually the polar measurement elements are determined with optical and electrooptical methods using the atmosphere as propagation medium. Optical inhomogenities in the propagation medium will cause refraction effects as beam bending and time-of-flight variations. They are considered as today's major source of systematic errors in the precise determination of angles and distances. Because direction transfer poses the highest requirements, in this paper we will concentrate on this topic.

2 REFRACTION ERRORS

2.1 Propagation model

According to the well-known Fermat-principle, light travelling from a source to a receiving system with the separation R describes exactly that path which is related to the shortest travel time. Due to the fact, that the light velocity depends on the refractive index of the propagation medium, the light from the emitter seeks the path r with the lowest refractive index. If the refractive index n varies perpendicular to the propagation direction ($\partial n/\partial y \neq 0$) the ray is bent; its deviation a from the original direction can be written as in equation (1a) [MORITZ, 1961]. Furthermore the complimentary angle b (see equation 1b), called the refraction angle in geodetic context, will be observed at the receiver.

$$\alpha = \frac{1}{R}\int_{r=0}^{R}(r-R)\frac{\partial n}{\partial y}dr\ , \qquad \beta = -\frac{1}{R}\int_{r=0}^{R} r\frac{\partial n}{\partial y}dr \tag{1 a,b}$$

Besides wavelength (see section 4), the refractive index depends on parameters describing the optical density; these are temperature and the partial pressures of the components of the propagation medium. The influence of temperature is the largest one, which amounts to approximately 1ppm/K. Because influence moisture and other additional components is diminutive, also their variation is neg-

ligible. The relatively small variation of dry air pressure is easy to model. So the spatial and temporal temperature changes are the most influential on the deviation from the straight line.

2.2 Orders of magnitude

The vertical temperature gradient can vary about ±1 K/m in layers near the ground, depending on season, daytime, type of surface, surface displacement etc. Furthermore, horizontal gradients occur, if the optical path runs along a surface, because its temperature influences air temperature. WILHELM [1994] reports that solar radiation on walls can produce gradients of several K/m in a distance of some decimeter, which gives a deviation of some centimeters for an optical path length of 100 m. For industrial application with error demands less than 10 µm, a temperature gradient of only 0.1 K/m produces a deviation, which exceeds the requirements, if the line of sight exceeds 15 m.

For practical example, in connection with the alignment tasks if the planned linear collider at DESY, Hamburg, Germany, with a total length of 32 km, the standard deviation of any point over a range of 576 m (Betatron-wavelength) should be better than 0.5 mm horizontally. But a constant temperature gradient of only 0.1 K/m perpendicular to the axis causes a maximum off-set of 4.5 mm for non-refraction compensated optical measurements. This is nine times the required adjustment standard deviation [SCHWARZ, 1997]. For tunnel boring tasks in connection with the Swiss Alptransit project HENNES et al. [1999] determined direction deviations ranging from 10 mm to 50 mm for one or two traverse legs of 500 m, even though sophisticated measurement set-ups have been considered. These calculations were based on preliminary temperature gradient measurement studies in the Swiss Albula tunnel.

2.3 Strategies for automated real-time elimination of refraction effects

An effective method for refraction compensation has to be in real-time and should avoid additional instruments as temperature sensors. Therefore, modules are envisaged, which are implemented in typical geodetic instruments as tacheometers or laser trackers. At present, we work on two different approaches. One approach bases on the additional information included in the stochastic properties of a light beam, which propagates through a turbulent medium using the effect, that the turbulence quantities are related to the refractive index gradient. In section 3, two measuring methods following this approach are introduced. The other approach bases on the dispersion effect to exclude the density dependence of the refractive index widely (see section 4).

3 TWO METHODS USING OPTICAL TURBULENCE

The effect, that the propagation of an electromagnetic wave is influenced by the turbulence of the atmosphere, can be used to derive atmospheric turbulence parameters. One possibility is the scintillation method, which bases on the determination of intensity fluctuation (also called scintillation) of a laser beam after its propagation through the turbulent atmosphere (see section 3.1), whereas thermally produced eddies influence the beam as well as mechanically produced ones. Another possibility is the analysis of image dancing (see section 3.3) which also is caused by the turbulent propagation medium. Both, the intensity fluctuation and the image dancing due to optical turbulence can be analyzed and with an atmospheric model several turbulence parameters can be derived. Section 3.2 gives a brief overview over the atmospheric model on which both methods are based on to derive the vertical refractive index gradient.

3.1 Scintillation method using a small aperture scintillometer

For the scintillation method, we use a displaced-beam scintillometer SLS20 [figure 1 and THIERMANN, 1992]. It is a small aperture scintillometer, which emits two parallel, differently polarized laser beams with the separation *d* and after their propagation over a path of 50 to 250 m, they are identified by their respective polarization at a receiver unit. During their propagation, the laser beams are scattered at refractive inhomogenities of the atmosphere and the intensity fluctuations can be measured as variance s_c^2 [LAWRENCE, STROHBEHN, 1970] and covariance B_{12} [THIERMANN, 1992].

$$\sigma_\chi^2(k,l_0,C_n^2) = 4\pi^2 k^2 \int_{r=0}^{R}\int_{\kappa=0}^{\infty} \kappa\Phi_n(\kappa,l_0,C_n^2)\sin^2\left[\frac{\kappa^2 r(R-r)}{2kR}\right]d\kappa dr \tag{2a}$$

$$B_{12}(k,l_0,C_n^2,a,d) = 4p^2k^2 \int_{r=0}^{R}\int_{k=0}^{\infty} k\Phi_n(k,l_0,C_n^2)J_0(kd)\sin^2\left[\frac{k^2 r(R-r)}{2kR}\right]\left[\frac{4J_1^2(kar/2R)}{(kar/2R)^2}\right]dkdr \tag{2b}$$

with

k	Wave number of radiation [m^{-1}]
$\Phi_n(k, l_0, C_n^2)$	Refractive index spectrum [m] [HILL, 1978]
J_0, J_1	Bessel functions
a	Aperture diameter

From the variance and the covariance of the intensity modulations of the received signals the structure function of the refractive index C_n^2 and the inner scale of turbulence l_o can be derived. From these two optical turbulence parameters it is now possible to determine the refractive index gradient.

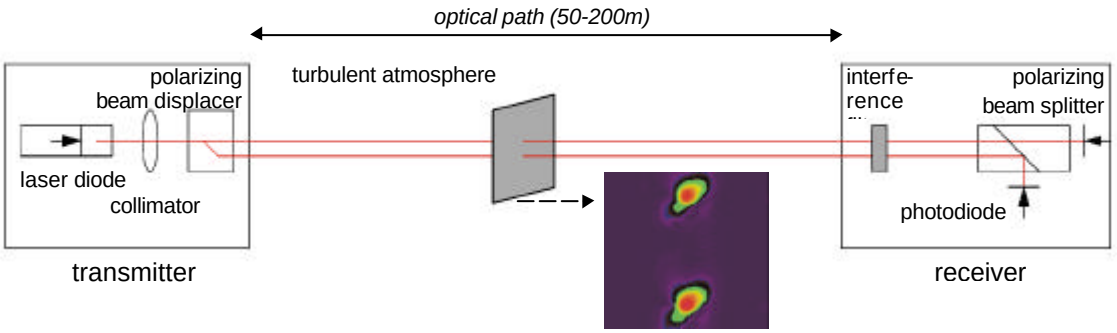

Figure 1: Simplified set up of the small aperture scintillometer SLS20

3.2 Atmospheric model for the derivation of optical turbulence parameters

The measurement with the small aperture scintillometer as well as the image dancing method deliver the turbulence parameters C_n^2 and l_o. From these two parameters the structure function of temperature C_T^2 on the one hand and the dissipation rate of turbulent kinetic energy e on the other hand can be obtained.

Based on the Monin-Obukhov turbulence theory the turbulent sensible heat flux H and the turbulent momentum flux M can be derived from C_T^2 and e. This is possible by setting up dimensionless equations for C_T^2 and e, which leads to the Obukhov Length L by a numerical iteration scheme. L is an indicator for the stability of the atmosphere, and is needed to determine the turbulent fluxes. Now it is possible to derive from the sensible heat flux the temperature gradient dT/dz and refractive index gradient dn/dz, which can be directly used to correct atmospheric induced errors in precise geodetic measurements. Figure 1 shows an example of the evolution of the refractive index gradient during a fair weather day with calm wind, measured on grass land at the Mesoscale Alpine Project (MAP) field campaign on the 25. Aug. 99. The figure shows a time series of 10 minutes averaged data for a height of one meter. It can be seen, that the refractive index gradient increases until noon and starts to decrease until the evening. The short, but strong decrease around 13:30 was caused by a cirrus cloud, which decreases the incoming solar radiation for about half an hour, with the result that also the refractive index gradient decreases. This curve indicates that the optical turbulence was mainly thermally produced on this day.

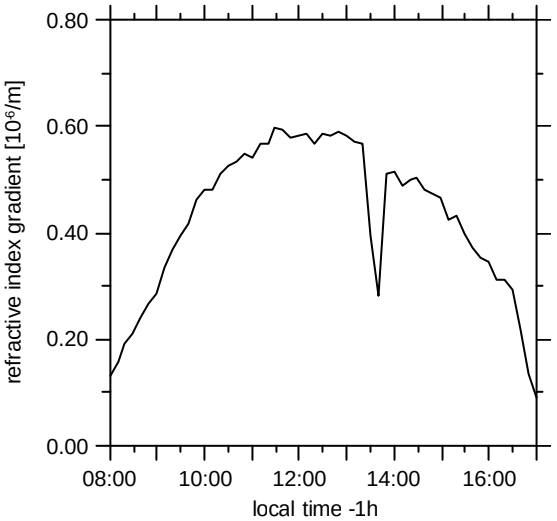

Figure 1: Time series of the refractive index gradient on the 25. Aug. 99, 10 min average, Riviera valley, Switzerland (10 min. average, z=1m)

3.3 Image dancing method using image processing

As mentioned above, image dancing can also be used to determine the turbulence parameters l_0 and C_n^2 which are necessary for the turbulence model. The required quantities can be measured by utilizing image processing. This dependence has been investigated in an experimental setup which consists of a digital line scan camera and a coded leveling rod.

3.3.1 Evaluation of phase fluctuations for determination of structure constant C_n^2

To determine the structure parameter C_n^2, the investigated approach uses the temporal changes of the vertical position y of image structures (edges) which can be measured by use of an appropriated edge operator. The standard deviation σ_y^2 of the positions of image structures is a measure for the fluctuation of the angle-of-arrival. The fluctuation of the angle-of-arrival is the result of refraction-induced phase fluctuations of light waves, arising when light beams propagate through a turbulent medium. Among a wide variety of formulae which are known for the determination of C_n^2, the approach of BRUNNER [1980] has provided plausible results, wherein σ_α^2 is the variance of angle-of-arrival [rad]:

$$C_n^2 = \frac{\sigma_\alpha^2 a^{1/3}}{1.05 \cdot R} \tag{3}$$

The variance of angle-of-arrival can be derived from the standard deviation of the σ_y^2 of the positions of the edges in the image (average) in dependence of pixel size p and focal length f

$$\sigma_\alpha^2 = \frac{\sigma_y^2 p^2}{f^2}. \tag{4}$$

3.3.2 Evaluation of intensity fluctuations for determination of inner scale l_0

This approach uses the dependence of the intensity fluctuations σ_I^2 of light waves propagating through a turbulent medium on the refractive index spectrum $\Phi_n(\kappa)$ where κ is the spatial frequency of the fluctuations. Hereby, the commonly used refractive index spectrum of HILL [1978] can be applied which is parameterized by l_0 and C_n^2. If this spectrum is integrated according (2a), the log-amplitude variance σ_χ^2 depends on l_0 and C_n^2. Moreover, the log-amplitude variance σ_χ^2 is related with the intensity fluctuations σ_I^2 per definition as follows:

$$\sigma_\chi^2 = \frac{1}{4}\ln\left(\sigma_I^2 + 1\right) \tag{5}$$

If the distance R, the wave number k of the radiation and the structure constant C_n^2 are known, a one-to-one relation between the intensity fluctuations σ_I^2 and the inner scale l_0 can be used in order to calculate the inner scale l_0 [FLACH, HENNES, 1998].

A crucial point in the method of image analysis is the derivation of an appropriate measure for the intensity fluctuations from the grabbed image data. In the scope of these experiments, the Wiener Filter [WIENER, 1950] has been evaluated since it provides a least-squares separation between the image signal (i.e. code pattern) and the noise which varies with the intensity fluctuations σ_I^2.

3.3.3 Experiment

This method has been practically investigated in various experiments, whereby a digital line scan camera with 1024 pixel and focal length of 500 mm grabbed the image of a coded leveling rod. The line scan rate was 330 Hz. Hence, it took about 10 s to grab 3000 lines which were compiled into an image.

Figure 3 shows the results of a field experiment in Claro (Switzerland) on a grass field with a line of sight of 74 m in a height of 1.5 m. A scintillometer (SLS 20) was positioned parallel to the line of sight to compare the results for C_n^2 and l_0 obtained by the line scan camera. The measurement series lasted about 5 hours. The temperatures amounted between 20°C at the beginning and reached a maximum of 27°C at 13:00. At about 11:30, clouds began to cover the sky.

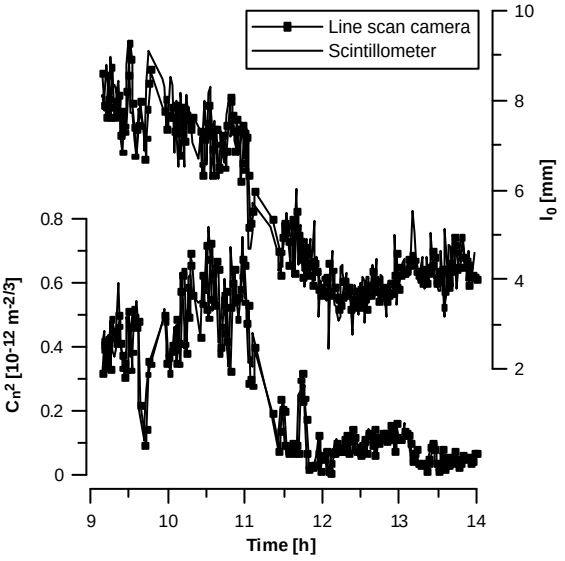

Figure 3: Comparison of results with Scintillometer (19. Aug. 1999, Claro, CH)

The results in figure 3 show a good correlation between the results of the line scan camera (dots) and the scintillometer (lines) for both C_n^2 and l_0. The correlation coefficient amounts to 0.9 for C_n^2 and 0.7 for l_0. The results must be considered under the aspect that the parameter C_n^2 and l_0 are subjected to rapid temporal changes. Furthermore, the method of image analysis can be limited if the

illumination of natural light is to weak (e.g. during night) or too strong (e.g. disturbing back light). Nevertheless, this methods is quite promising for the determination of C_n^2 and l_0 and, finally, the vertical refractive index gradient can be derived according section 3.2.

4 THE DISPERSION METHOD

The dispersion method is a purely metrological solution to atmospherically induced limitations in very high-accuracy optical direction measurements and alignment tasks.

4.1 Theory of the method

The principle of the dual-wavelength method utilizes atmospherical dispersion, i.e. the wavelength dependence of the refractive index (see figure 4). The difference angle between two light beams of different wavelengths, which is called the dispersion angle $\Delta\beta$, is to first approximation proportional to the refraction angle:

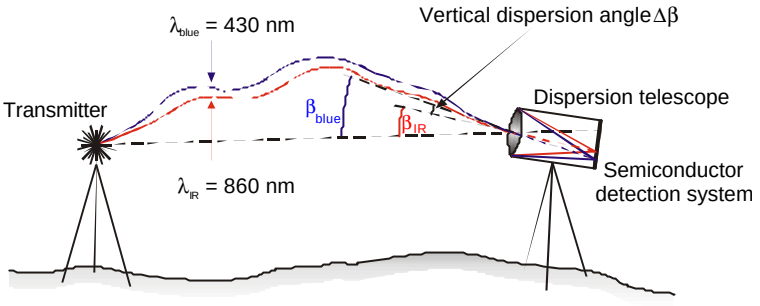

Figure 4: Dispersometer-principle

$$\beta_{IR} = \nu(\beta_{blue} - \beta_{IR}) = \nu\Delta\beta \qquad (6)$$

herein shown for the refraction angle β_{IR} for the IR-radiation. Furthermore β_{blue} in equation (6) denotes the refraction angle for blue light. The wavelength dependent constant ν, calculated by using a dispersion formula has the magnitude of ~42 for the presently used wavelengths. This implies that the dispersion angle has to be measured at least 42 times more accurate than the desired accuracy of refraction angle. This required accuracy constitutes the major difficulty for the instrumental performance in applying the dispersion method. Further major difficulties in instrumental realization arise in the availability of a suitable dual-wavelength laser light source and stable coaxial emittance of monomode radiation at both wavelengths.

The initial quantity of observation, the dispersion angle, appears as a displacement between the centers of gravity of the imaged intensity distributions of both wavelengths on the semiconductor detection system in the focal plane of the dispersion telescope. With known focal length f of the telescope one can calculate the vertical dispersion angle $\Delta\beta$. And thereof using equation (6) finally the refraction angle β_{IR} at the IR-wavelength can be obtained. A more detailed analysis can be found in [INGENSAND, BÖCKEM, 1997].

4.2 Instrumental approach of the dispersometer

Modern geodetic total-stations can be characterized as multi-laser- and multi-sensor-systems. Arising from this fact, we are currently developing a dispersometer as an additional dual-laser/sensor-system, which can be implemented into existing total-stations exploiting their full accuracy-potential. According to the dual-wavelength method the dispersometer consists of two modules: the dual-wavelength transmitter and the detector module being composed of a dispersion telescope and a semiconductor detection system (see figure 4).

The core of the dual-wavelength transmitter is the dual-wavelength laser generating blue light by frequency doubling of the wavelength of a semiconductor IR-laser diode in a potassium niobate ($KNbO_3$)-crystal. Such an all-solid-state laser is ideally suited for the dual-wavelength transmitter and leaves out the problem of beam combining. Furthermore, with the implementation of a modulator and the application of optical fiber technology we demonstrated in the recent set-up of the dual-wavelength transmitter: dual-wavelength laser light generation, laser light modulation with a very high extinction ratio and stable coaxial monomode propagation at both wavelengths with sufficient optical power for field applications [BÖCKEM, 1999]. Beyond this, the dual-wavelength transmitter can be coupled into one optical channel of a high-end geodetic total-station.

After propagating through the atmosphere both beams are collected by an especially calculated dispersion telescope with a focal length of 300 mm. Consequently, this dispersion telescope can be compared with an ordinary telescope of a high-end theodolite as far as the focal length is concerned. The maximum aperture of 75 mm can be reduced continuously for analyzing the functional dependence of the sensitivity of the turbulence compensation mechanism on the aperture size.

By the assumption of a refraction angle in the order of 1µrad, related to the dual-wavelength theory, the magnitude of the wavelength dependent constant n implies that the dispersion angle has to be

resolved better than 0.03 µrad. This angular value is equivalent to the resolution on the sensor of 10 nm with the consideration of a predetermined focal length of 300 mm of the optical system. Although the used types of position sensitive detector (PSD) are segmented photodiodes, either the dual- or the quad-cell type, the gap in between the actually sensitive areas, performing as a lateral detector, is utilized to obtain highest resolution of position.

The proposed dispersometer is designed to overcome the aforementioned difficulties in instrumental realization. Hence, it will be capable of true, i.e., refraction free direction measurements and direction transfers, the detrimental influence of atmospheric turbulence notwithstanding.

5 CONCLUSIONS AND OUTLOOK

The results of the scintillation method are promising in respect to calculate real-time corrections for the beam bending, which are valid for the whole path length, because the data gives line-averaged values. New studies are being pursued, which examine the possibility of utilizing the data acquisition features of common surveying instruments. Up to now, the modeling of turbulence is in principle restricted to a horizontal homogenous surface, because it is based on Monin-Obukov theory, but that problem is presently being investigated. However, the only method working without restrictions constitutes dispersometry. Therefore, the high technological effort for a working dispersometer is justified. However, because of the sophisticated instrumental set-up, the dispersion method will be restricted to specific applications with very high accuracy demands.

REFERENCES

BÖCKEM, B. [1999]: High-Accuracy Alignment Based on Atmospherical Dispersion – Technological Solutions for the Dual-Wavelength Transmitter. IWAA99, Oct. 18.-21.1999, Grenoble, France.

BRUNNER, F.K. [1980]: Systematic and Random Atmospheric Refraction Effects in Geodetic Levelling. Proc. of Second International Symposium on Problems Related to the Redefinition of North American Vertical Geodetic Networks, Ottawa (Canada), pp. 691-703.

FLACH, P., HENNES, M. [1998]: Die optische Turbulenz - wirklich nur ein limitierender Faktor für geodätische Messungen? In: Freeden W. (ed.): Progress in Geodetic Science, Proceedings to Geodätische Woche Kaiserslautern 1998, pp. 65-72.

HENNES, M., DÖNICKE, R., CHRIST, H. [1999]: Zur Bestimmung der temperaturgradienteninduzierten Richtungsverschwenkung beim Tunnelvortrieb. VPK, 8/99, pp. 418-426.

HILL, R. J., CLIFFORD, S. F. [1978]: Modified spectrum of atmospheric temperature fluctuations and its application to optical propagation. Journal of the Optical Society of America, Vol. 68 (7), pp. 892-899.

INGENSAND, H., BÖCKEM, B. [1997]: A High-Accuracy Alignment System Based on the Dispersion Effect. IWAA97, Oct. 13.-17.1997, Argonne, IL.

LAWRENCE, R. S.; STROHBEHN, J. W. [1970]: A Survey of Clear-Air Propagation Effects Relevant to Optical Communications. Proceedings of the IEEE, Vol. 58, No. 10/1970, pp. 1523-1545.

MORITZ, H. [1961]: Zur Reduktion elektronisch gemessener Strecken und beobachteter Winkel wegen Refraktion. ZfV, pp. 246-252.

SCHWARZ, W. [1997]: Concept for the Alignment of the planned Linear Collider at DESY. IWAA97, Oct. 13-17, 1997, Argonne, IL.

THIERMANN, V. [1992]: A displaced-beam scintillometer for line-averaged measurements of surface layer turbulence, 10th Symposium on Turbulence and Diffusion, 29. Sept.-2. Oct. 1992, Portland, OR.

WIENER, N. [1950]: Extrapolation, Interpolation, and Smoothing of Stationary Time Series. New York, Wiley.

WILHELM, W. [1994]: Die Seitenrefraktion - Ein unbeliebtes Thema? Oder ein Thema nur für Insider? VPK 2/94, pp. 75-82.

AUTHORS: Dipl.-Ing. B. BÖCKEM, Dipl.-Ing. P. FLACH, Dr. M. HENNES, Institute of Geodesy and Photogrammetry, ETH Zürich, Hönggerberg, CH-8093 Zürich, Switzerland, phone +41-1-633 3044/3605/3041, fax –1101, E-mail: {boeckem,flach,hennes}@geod.baug.ethz.ch

Dipl.-Met. A. WEISS, Institute of Geography, ETH Zürich, Winterthurerstr. 190, CH-8057 Zürich, Switzerland, phone +41-1-635 5208, E-mail: weiss@geo.umnw.ethz.ch